

Hydrodynamic Isotonic Fluid Delivery Ameliorates Moderate-to-Severe Ischemia-Reperfusion Injury in Rat Kidneys

Jason A. Collett,* Peter R. Corridon,† Purvi Mehrotra,* Alexander L. Kolb,‡
George J. Rhodes,§ Caroline A. Miller,|| Bruce A. Molitoris,§,¶ Janice G. Pennington,||
Ruben M. Sandoval,§ Simon J. Atkinson,‡ Silvia B. Campos-Bilderback,§ David P. Basile,*§
and Robert L. Bacallao§**

*Department of Cellular and Integrative Physiology, §Division of Nephrology, Department of Medicine, ¶Department of Anatomy and Cell Biology, and ||Indiana Center for Biological Microscopy, Indiana University School of Medicine, Indianapolis, Indiana; †Department of Craniofacial Biology, University of Colorado Denver, Anschutz Campus, Aurora, Colorado; ‡Department of Biology, Indiana University–Purdue University, Indianapolis, Indiana; and **Department of Medicine, Division of Nephrology, Richard L. Roudebush Veterans Affairs Medical Center, Indianapolis, Indiana

ABSTRACT

Highly aerobic organs like the kidney are innately susceptible to ischemia-reperfusion (I/R) injury, which can originate from sources including myocardial infarction, renal trauma, and transplant. Therapy is mainly supportive and depends on the cause(s) of damage. In the absence of hypervolemia, intravenous fluid delivery is frequently the first course of treatment but does not reverse established AKI. Evidence suggests that disrupting leukocyte adhesion may prevent the impairment of renal microvascular perfusion and the heightened inflammatory response that exacerbate ischemic renal injury. We investigated the therapeutic potential of hydrodynamic isotonic fluid delivery (HIFD) to the left renal vein 24 hours after inducing moderate-to-severe unilateral IRI in rats. HIFD significantly increased hydrostatic pressure within the renal vein. When conducted after established AKI, 24 hours after I/R injury, HIFD produced substantial and statistically significant decreases in serum creatinine levels compared with levels in animals given an equivalent volume of saline via peripheral infusion ($P < 0.05$). Intravital confocal microscopy performed immediately after HIFD showed improved microvascular perfusion. Notably, HIFD also resulted in immediate enhancement of parenchymal labeling with the fluorescent dye Hoechst 33342. HIFD also associated with a significant reduction in the accumulation of renal leukocytes, including proinflammatory T cells. Additionally, HIFD significantly reduced peritubular capillary erythrocyte congestion and improved histologic scores of tubular injury 4 days after IRI. Taken together, these results indicate that HIFD performed after establishment of AKI rapidly restores microvascular perfusion and small molecule accessibility, with improvement in overall renal function.

J Am Soc Nephrol 28: •••–•••, 2017. doi: 10.1681/ASN.2016040404

Ischemia-reperfusion (I/R) injury to the kidney has the potential to result in significant damage and loss of renal function. The loss of GFR after I/R injury is due in part to multiple factors, including damage to renal tubules, which have been proposed to increase intraluminal pressures and negatively influence net filtration.¹ I/R injury can compromise vascular function leading to reduced renal blood flow and alterations in microvascular perfusion patterns.^{1–4} The resultant effects of impaired vascular function in the setting of I/R are at least

two-fold. First, increased renal vasoconstriction reduces net glomerular hydrostatic pressure to reduce GFR. Second, impaired perfusion distribution

Received April 6, 2016. Accepted December 17, 2016.

Published online ahead of print. Publication date available at www.jasn.org.

Correspondence: Dr. Robert L. Bacallao, Indiana University Medical Center, Research II, Suite E202, 950 W Walnut Street, Indianapolis, IN 46202-5188. Email: rbacalla@iu.edu

Copyright © 2017 by the American Society of Nephrology

through the postglomerular vasculature may exacerbate the degree of hypoxia thus sustaining or exacerbating the degree of tubular damage.¹

To date, treatment of patients with AKI is limited primarily to supportive care, by maintaining extracellular fluid volume and electrolyte balance over a critical period during which endogenous processes may mediate injury resolution and repair of damaged tissue.⁵ However, there has been no significant advance in therapies to treat patients with established AKI, either to improve function or facilitate repair processes. Given the importance of renal perfusion in the pathophysiology of I/R-induced AKI, there has been significant attention on potential treatments designed to improve renal blood flow to mitigate AKI. Although vasodilators have shown efficacy in AKI prevention in animal models,⁶ these therapies have not translated to effective clinical therapy as noted by the failure of renal dose dopamine to improve AKI.⁷

In recent years, the concept of the extension phase of AKI has been articulated, in which postischemic activation of an inflammatory process results in vascular congestion.³ Significant evidence exists that I/R-induced expression of surface adhesion molecules, such as ICAM-1, on the endothelium promotes leukocyte adhesion. Adherent leukocytes contribute to renal injury by impairing perfusion and by production of cytokines, which enhances inflammatory responses, further promoting tissue damage. The no-reflow phenomenon contributes to AKI in animal models and impaired microvascular perfusion associated with red cell congestion can be readily imaged *in vivo* using light microscopy.^{3,8,9} Yamamoto *et al.* demonstrated that endothelial dysfunction was a primary contributor to microvascular flow distortions after I/R injury.⁴ Wu *et al.* and more recently Nakano *et al.* used intravital light microscopy to demonstrate reduced capillary blood flow and tubule fluid flow in an LPS injury model.^{10,11}

Vascular congestion distal to the efferent arteriole vasculature may be a primary factor in reducing perfusion and driving the extension phase. Leukocyte adhesion is prominent in the

postischemic kidney primarily with low hydrostatic pressure. Therefore, it is reasonable to search for treatments geared toward reducing vascular congestion in capillaries and venules. Because increasing hydrostatic pressure perturbs leukocyte adhesion, an elevation of pressure in regions may clear existing congestion and help to re-establish effective perfusion. Renal vein hydrodynamic isotonic fluid delivery (HIFD) effectively administers macromolecules to the kidney for use in exogenous gene expression.¹² This process may be dependent on an increase in intravascular pressure focused transiently at the level of the peritubular capillary network.¹² Because of this, we hypothesized that renal vein HIFD may effectively reverse established I/R-induced AKI by re-establishing renal perfusion. We evaluated this hypothesis by investigating HIFD treatment after establishment of AKI in rats.

RESULTS

Correlative Light and Electron Microscopy of I/R-Injured Kidneys

In prior reports, intravital light microscopy studies found microvascular changes in white cell adhesion in the setting of I/R injury.¹³ In addition to changes in white cell adhesion to the endothelium, red cell stacks identified as large negatively stained areas are readily observed in a 24 hours postischemic kidney (Figure 1, arrows). The extended size and relative lack of movement of these structures suggested that rouleaux were causing microvascular occlusion in the postischemic kidneys. To confirm, we performed a correlative experiment in which a region of interest (ROI) identified by intravital light microscopy was sampled by biopsy, followed by rapid freeze fixation to evaluate ultrastructural changes observed at light microscopy resolution. Figure 1A illustrates the presence of aggregate of red blood cells occluding the capillary lumen by light microscopy, whereas Figure 1B illustrates the same region at ultrastructural resolution. Figure 1C illustrates capillary cross

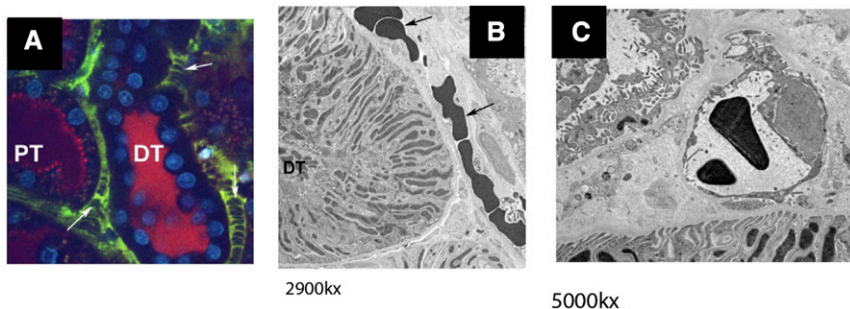


Figure 1. Rouleaux formation within the renal microvasculature after renal I/R. (A) Multiphoton imaging of renal microcirculation was conducted using 150 kD FITC dextran 24 hours after renal I/R injury; vascular congestion and stacked red blood cells are evident in the cortical microvasculature after I/R (white arrows). (B) Electron microscopy of the highlighted region in (A) after correlative tissue sampling and subsequent cryofixation after high-pressure freezing demonstrating red blood cell congestion in peritubular capillaries (arrows). (C) Capillary cross section in a control, nonischemic kidney. Sample was cryofixed after high-pressure freezing. Magnifications are listed below electron micrographs. DT, distal tubule; PT, proximal tubule.

section with a nonoccluding red cell as commonly observed in control, nonischemic kidneys. These observations are consistent with long-standing observations of vascular congestion observed macroscopically in postischemic kidneys.^{14–16}

Hydrodynamic Delivery of Saline via the Renal Vein Is Sufficient to Ameliorate the Course of AKI

HIFD effectively delivers macromolecules to cells in kidneys.¹² The combination of a pressurized transient fluid injection results in permissive fluid passage through fenestrated endothelium and may disrupt vascular congestion directly.¹²

To test the effect of HIFD on the course of AKI, I/R injury was induced by right unilateral nephrectomy and left renal pedicle cross clamp in rats. At 24 hours post-I/R, plasma creatinine levels were measured and rats were subjected to either renal HIFD into the left renal vein or a control injection of an equivalent saline volume into the vena cava. Rats were allowed to recover for an additional 1 or 3 days (*i.e.*, 2 or 4 days post-I/R). HIFD resulted in a transient increase in renal venous pressure from approximately 6.5 to 66.5 ± 6 mmHg (Figure 2A). HIFD eliminated regions of hypoperfusion readily observable grossly in a post-ischemic kidney (Figure 2B, left panel, arrows, compared with the right panel). In both 2- and 4-day cohorts of vena cava-injected rats, the plasma creatinine values continued to rise between 24 and 48 hours, whereas rats subjected to renal vein HIFD manifested a significant decline in plasma creatinine (Figure 2, C and D). Indeed, when combining data from all rats, the change in plasma creatinine between 24 and 48 hours was improved in HIFD-treated rats by 1.65 ± 0.34 mg/dl (Figure 2E). This procedure was also associated with a significant acceleration in recovery of renal morphology as illustrated by the improvement in renal tubular damage present at 4 days after I/R in HIFD- versus vena cava-treated rats (Figure 2, F–H).

Hydrodynamic Delivery of Saline via the Renal Vein Re-Establishes Capillary Perfusion Post-I/R Injury

Renal histology shown in Figure 2F demonstrated the sustained presence of red blood cells (RBCs) in renal capillaries in vena cava-injected post-AKI rats (Figure 2F, black arrows), whereas rats showed a significant reduction in RBCs after HIFD (Figure 2, F–I). Therefore, we hypothesized that HIFD may accelerate recovery by improving renal perfusion. To investigate further HIFD effects, we performed intravital light microscopy on kidneys 24 hours after I/R injury immediately before and immediately after HIFD therapy. In keeping with prior studies, we found areas of hypoperfusion corresponding to regions where red cell ghosts are seen consistent with rouleaux (Figure 3B, Supplemental Movies 1 and 2). Imaging the same kidney after HIFD revealed improved capillary bed perfusion with less observable rouleaux (Figure 3C, Supplemental Movie 1). Analysis of RBC velocity suggested that renal I/R resulted in an approximately 81% reduction in microvascular perfusion relative to sham-operated control rats. RBC velocity, although still suppressed versus sham, was significantly improved 2.3-fold by HIFD by within 30 minutes of the procedure (Figure 3D).

In addition to improvements in microvascular perfusion, an unexpected result revealed by these studies came from the use of Hoechst 33342, which is routinely included in intravital light microscopy studies to label nuclei. Hoechst 33342 has a mol wt of 452 g/mol and it efficiently labels cell nuclei because of its cell permeant properties.¹⁷ Its size is equivalent to the mol wt of small molecule therapeutic agents. Figure 3B illustrates that Hoechst 33342 nuclear labeling is weak as compared with sham (Figure 3A), with an average fluorescent intensity of 20.12 ± 2.8 (Figure 3E). After HIFD, nuclear labeling is stronger (Figure 3C, arrows) and average fluorescence intensity measurement of nuclei was significantly enhanced (Figure 3E; 73.2 ± 1.1 ; $P < 0.05$). Notably, Hoechst 33342 was injected *via* the tail vein when the experimental preparation was started. No additional Hoechst 33342 was given during the study, so the change in nuclear staining likely reflects improved microvascular perfusion allowing label to enter cells. To eliminate the possibility that HIFD treatment disrupts vascular permeability, we modified our experimental procedure where 150 kD tetramethyl rhodamine isothiocyanate (TRITC)-conjugated dextran was injected *via* tail vein, 20 minutes after HIFD. The animals had a right nephrectomy with contralateral I/R injury 24 hours before HIFD therapy. Image collection in a single plane over time was performed to assess diffusion of the high-mol wt fluorescent probe into the interstitial space. Figure 3F shows that there is no change in vascular permeability between pre- or post-HIFD-treated kidneys. Hoechst 33342 given concomitant with the high-mol wt dextran, both given by a peripheral intravenous infusion, is now able to label nuclei, confirming that HIFD improves delivery of Hoechst 33342 to cells by re-establishing capillary perfusion and not by altering vascular permeability.

Hydrodynamic Delivery of Saline via the Renal Vein Reduces Inflammatory Cell Infiltration Post-I/R Injury

To determine if HIFD reduced infiltration of leukocytes, we measured mononuclear cell populations 2 days after I/R. We observed that I/R injury increased the total number of mononuclear cells, infiltrating CD4+ or CD8+ lymphocytes, CD4+17+, CD8+IL-17+ cells, B cells, and dendritic cells/macrophages (DC/Macs) compared with sham ($P < 0.05$). Interestingly, total mononuclear cell number, CD4+ or CD8+ lymphocytes, CD4+17+, CD8+IL-17+ cells, B cells, and DC/Macs were all significantly reduced after HIFD ($P < 0.05$). Neither AKI nor HIFD had an effect on Th1 or Th2 polarization (Figure 4, Table 1).

In addition, T regulatory cells are associated with modulating T cell activity after renal injury.¹⁸ Interestingly, within 2 days of I/R injury, the percentage of CD4+Foxp3+ cells was significantly greater in HIFD-treated rats compared with vena cava-treated rats (Table 1).

Efficacy of HIFD in the Absence of Renal Artery Clamping

To test whether HIFD may translate to clinical settings using intravascular approaches, we repeated the HIFD studies without clamping the renal artery during the perfusion. Although a kidney

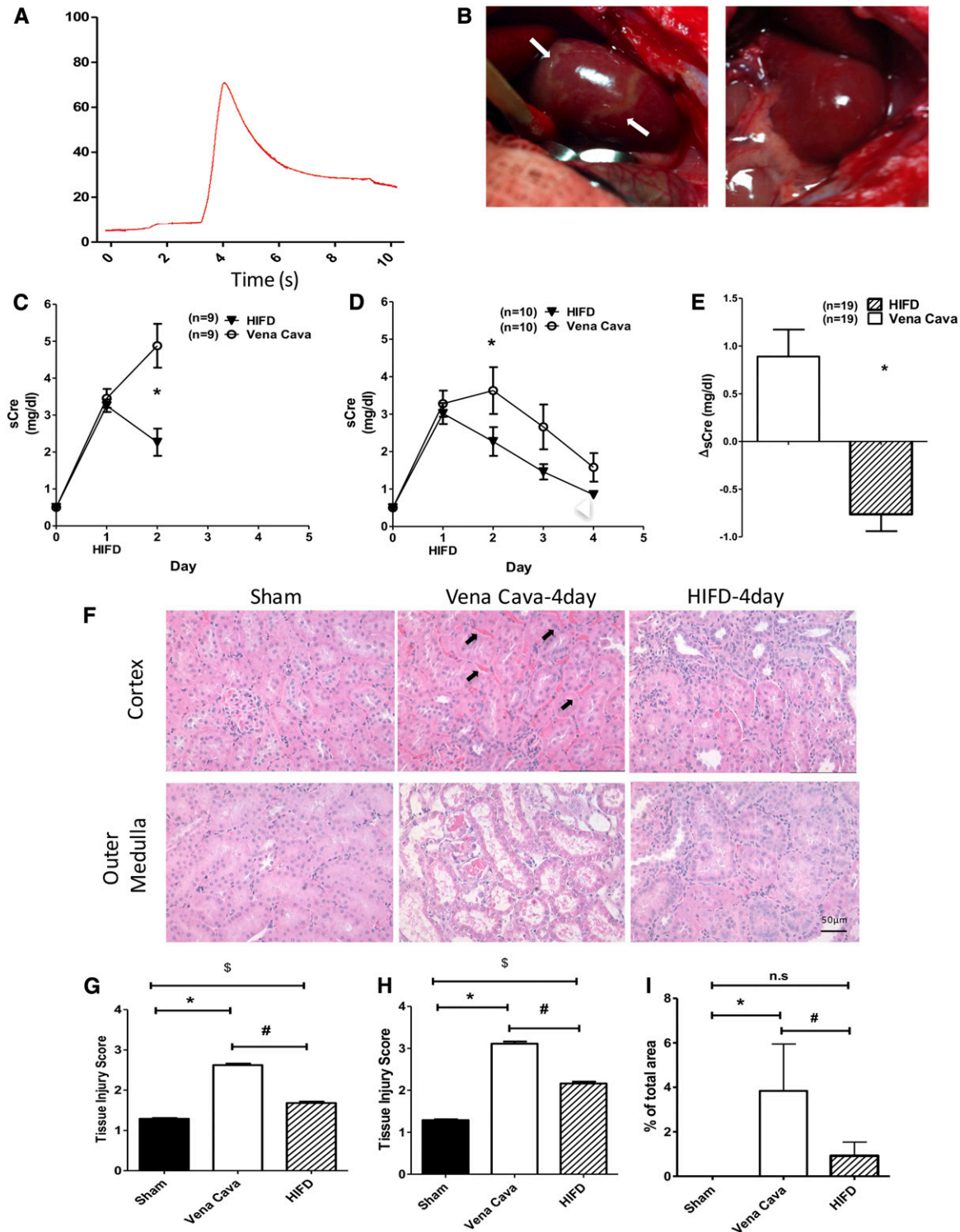


Figure 2. HIFD improves renal function and structure post-AKI. Rats were subjected to unilateral nephrectomy and unilateral I/R and allowed to recover for 24 hours before HIFD or vena cava saline infusion. (A) Representative tracing of renal venous pressure during HIFD, (B) (left panel) gross images of post-AKI kidney before, and (B) (right panel) 3 minutes after HIFD in the same kidney. Note elimination of striated zones of hypoperfusion post-HIFD (left panel, arrows). (C and D) Serum creatinine (sCre) versus time after HIFD or vena cava injection 24 hours post-I/R in rats recovering for 2 days (C) or 4 days (D) postsurgery. (E) Change in serum creatinine in the 24-hour period immediately after HIFD in all 2- and 4-day-treated rats (A–E); *N* for each group is shown at each time point; **P*<0.05 in HIFD versus vena cava by unpaired *t* test. (F) Representative renal histology 4 days post-I/R. Cross sections of hematoxylin and eosin stained cortex and

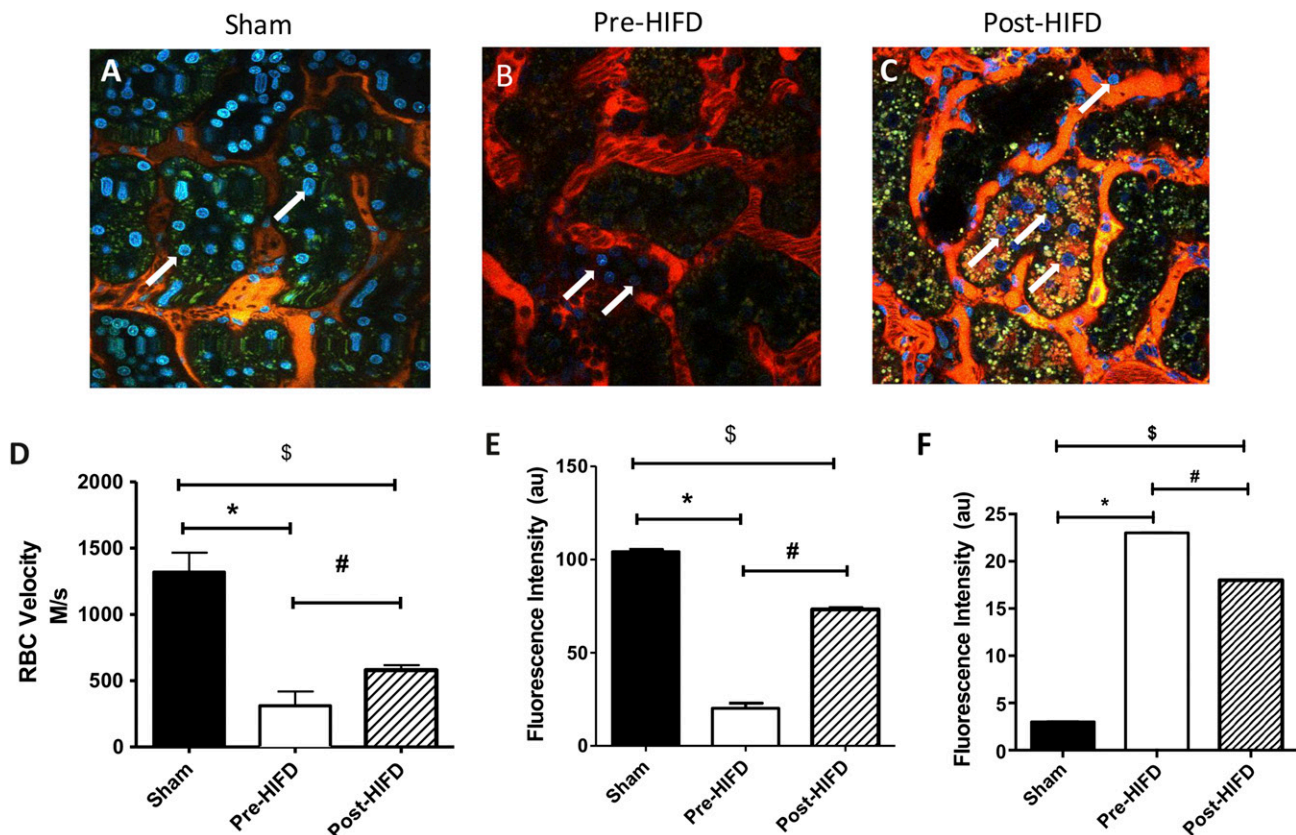


Figure 3. HIFD immediately improves vascular congestion in a post-AKI kidney. Live multiphoton imaging of sham kidney (A) or kidneys 24 hours post I/R, immediately before (B) and 30 minutes post-HIFD injection (C) are shown. (D) A line scan was generated and is indicative of average RBC velocity in the capillary space pre- and post-HIFD injection. (E) Average nuclear fluorescent intensity of Hoechst 33342 signal in tubular epithelial cells pre- and post-HIFD; for (D) and (E), data are mean \pm SEM of fluorescent intensity (arbitrary units) of 10 ROI of images from three separate experiments for sham or pre- and post-HIFD. (F) Fluorescent intensity per unit time in sham versus pre- and post-HIFD-treated rats. Fluorescent intensity (arbitrary units) of the interstitial space fluorescence as a percentage of tubule fluorescence of 10 ROI of images from three separate experiments. *\$P<0.05 for sham versus *pre-HIFD or versus \$post-HIFD using paired t test; #P<0.05 for pre-HIFD versus post-HIFD using paired t test.

hydrodynamic pulse is feasible with a renal vein catheter, simultaneous renal artery and venous cannulation would probably exacerbate kidney ischemia and is technically difficult. Therefore, we conducted an additional study to test the efficacy of HIFD in the absence of renal artery clamping. Similar to observations in the presence of renal pedicle clamping, HIFD without renal artery clamping also resulted in significant reduction in serum creatinine (Figure 5A). Comparing serum creatinine at day 2 to day 1, the change in serum creatinine for HIFD-treated animals was -0.33 . In contrast, the change in serum creatinine for animals given saline *via* the vena cava was 1.51 . There are significant reductions in infiltrating inflammatory cells, CD4, and CD8 cells in HIFD animals (Figure 5, B and C). IL17-positive cells were also

diminished in HIFD-treated animals (Figure 5D) and subtype studies showed that CD4+/IL17+ and CD8+/IL17+ cells both decreased in HIFD-treated animals as well (Figure 5, E and F). Finally, we also found that HIFD performed with the renal vein occluded restored capillary blood flow to the same degree as HIFD performed with artery and vein occlusion (Figure 5G).

DISCUSSION

AKI is a syndrome characterized by the rapid loss of the kidney's excretory function leading to unacceptably high morbidity and mortality.¹ The rapid decline in renal function is

outer medulla from sham, I/R + vena cava injection, or I/R + HIFD in cortex are shown. Black arrows indicate congested RBCs in peritubular capillaries. (G and H) Renal injury scores on the basis of renal histology of kidney tissue ([G] cortex; [H] outer medulla) from (F). (I) Quantification of cortical vascular congestion expressed as percentage of total area from (F). (G–I) *\$P<0.05 for sham versus *I/R + vena cava or \$I/R + HIFD; #P<0.05 for I/R + vena cava versus I/R + HIFD by paired t test. *P<0.05 in HIFD versus vena cava by unpaired t test.

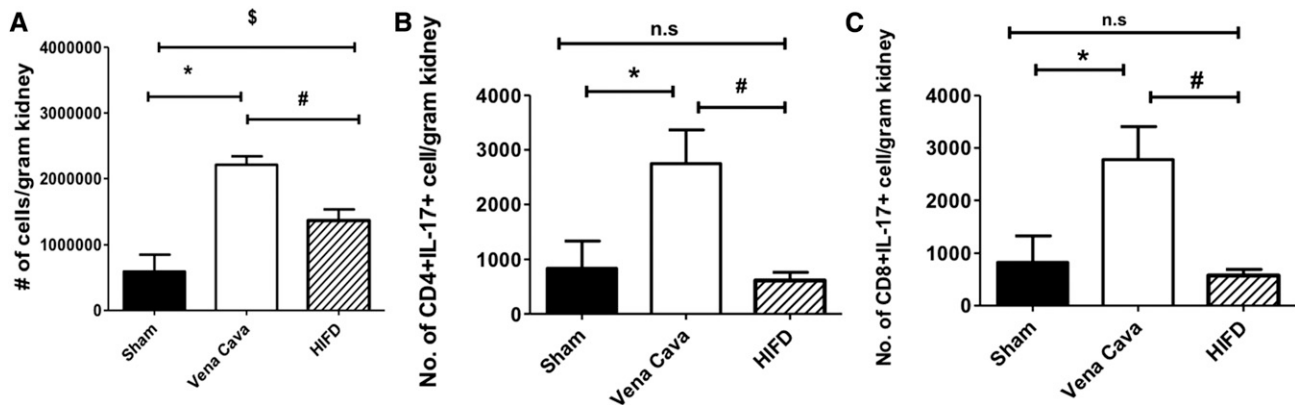


Figure 4. HIFD reduces the number of infiltrating inflammatory cells 48 hours postsurgery. Kidneys from rats after sham surgery, I/R + vena cava, or I/R + HIFD 2 days after surgery were used for isolation of monocytes and FACS for the following populations: (A) total number of infiltrating cells, (B) IL17⁺CD4⁺ cells, and (C) IL17⁺CD8⁺. Data are expressed as mean \pm SEM number of cells per gram kidney weight; *\$P<0.05 for sham versus *I/R + vena cava or \$I/R + HIFD; #P<0.05 for I/R + vena cava versus I/R + HIFD by paired t test.

associated with decreased renal perfusion, tubular necrosis, and damage to the glomeruli, interstitium, and vasculature. Although the tubules are a major target of injury as indicated by severe morphologic damage, endothelial dysfunction contributing to vascular congestion and inflammation represent principal components of the extension phase of injury. This extension phase, described by Sutton and Molitoris, recognizes that impaired perfusion post-AKI may exacerbate hypoxia and result in greater tubular damage than would be seen if perfusion remained intact.^{3,13} It has been suggested that targeting the extension phase may represent a significant advance in the treatment of AKI,³ however, to date there have been no Food and Drug Administration-approved available treatments which have shown significant efficacy in targeting these activities. The components of the extension phase are more pronounced in the outer medullary region of the kidney, where reduced blood flow, stasis, and accumulation of red and white cells is most prominent.^{1,19,20} It is during this phase that renal vascular endothelial cell damage likely plays a key

role in the inflammatory response observed with ischemic AKI.¹ Inflammatory cell infiltration is a prominent early feature in the outer medullary vasa recta capillaries after injury. Animal models of AKI show that ischemic injury is accompanied by the rapid influx of leukocytes, lymphocytes, dendritic cells, and macrophages into the interstitium.^{21–23} Particularly, there is growing evidence supporting an important role of T cells in AKI.^{24–28} How T cells promote injury is still under investigation, however, it is possible that this activity is secondary to alterations in the endothelium. Endothelial cells have a significant increase in surface expression of leukocyte adhesion molecules such as ICAM-1, along with P- and E-selectin, in response to injury.^{29–31} Treatments geared toward reducing endothelial/leukocyte interactions by targeting these endothelial adhesion molecules preserve blood flow and protect against renal damage in ischemic AKI in preclinical models of renal I/R.^{30,31} Interestingly, whereas studies in transplant suggest that anti-ICAM-1 may prevent AKI, other studies using ICAM-1 demonstrate no effect after AKI was established in settings such as in toxic AKI.^{32,33}

Vascular congestion is an important feature contributing to the severity of AKI.^{1,13,29,34,35} Ischemia causes the upregulation of genes such as ICAM-1 and vascular cell adhesion protein 1 and the downregulation of the endothelial glycoprotein thrombomodulin.^{22,36} A combination of activated leukocytes binding to adhesion molecules, endothelial damage, and platelet aggregation leads to microvascular congestion and reduced perfusion.^{2,19,37} After the reduction in renal perfusion, epithelial cells are unable to maintain intracellular ATP leading to cell injury, potentially leading to apoptosis or necrosis.¹⁹ That RBC congestion plays a critical role in the genesis of tubular injury and loss of renal function is supported by studies from Hellberg and Olof *et al.* demonstrating that a reduction in the hematocrit reduced post-ischemic erythrocyte congestion, and improved GFR and renal morphology.^{35,38}

Table 1. Effect of HIFD on infiltrating inflammatory cells 2 days post-I/R injury

Cell Type	Treatment		
	Sham	Vena Cava	HIFD
CD4+	6272 \pm 3839	21,101 \pm 4198 ^a	9987 \pm 2964 ^b
CD8+	5097 \pm 4506	15,444 \pm 2637 ^a	8474 \pm 1468 ^b
B cells	2351 \pm 1510	5743 \pm 1609	2868 \pm 880 ^b
DC/Macs	12,695 \pm 5433	34,684 \pm 7758	21,495 \pm 3880 ^b
CD4+IL-4+ (Th1)	161 \pm 58	280 \pm 52.8	200 \pm 50
CD4+IFN- γ + (Th2)	277 \pm 82	1301 \pm 667	399 \pm 113
% CD4+Foxp3+	0.7 \pm 0.01	0.405 \pm 0.04	0.72 \pm 0.08 ^b
% CD8+Foxp3	0.35 \pm 0.1	0.15 \pm 0.02 ^a	0.29 \pm 0.06

The table shows different subtypes of infiltrating mononuclear cells in the kidney 48 hours postinjury in sham, I/R + vena cava, or I/R + HIFD. The data are shown as the number of cells/g of kidney. Data are expressed as mean \pm SEM.

^aP<0.05 sham versus I/R + vena cava.

^bP<0.05 in I/R + vena cava versus I/R + HIFD.

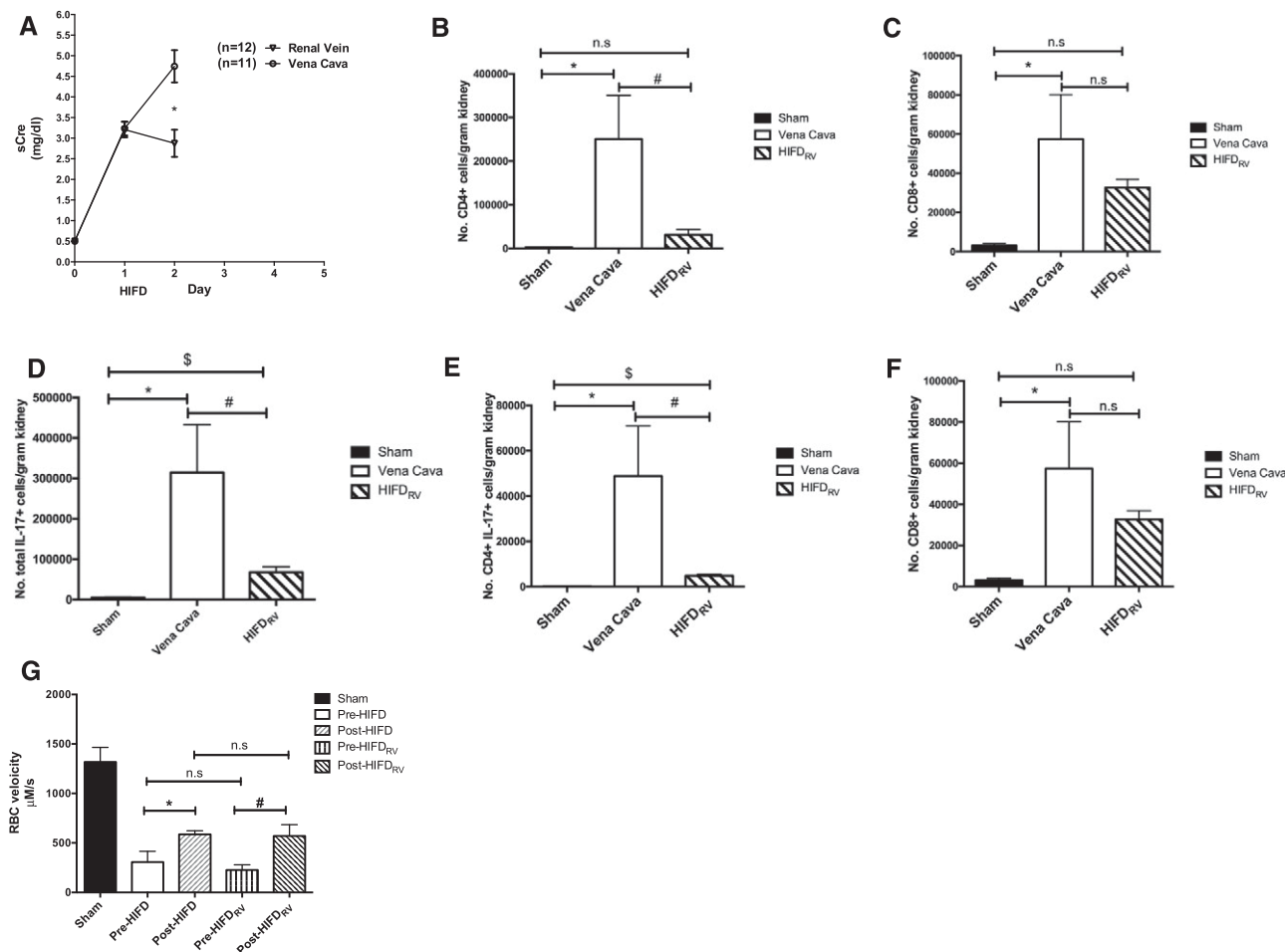


Figure 5. HIFD_{RV} improves renal function, reduces the number of inflammatory cells, and improves microvascular perfusion. Rats were subjected to unilateral nephrectomy and unilateral I/R and allowed to recover for 24 hours before HIFD or vena cava saline infusion. In contrast to initial studies, only the renal vein was occluded before and during HIFD (HIFD_{RV}). (A) Serum creatinine versus time after HIFD_{RV} or vena cava injection 24 hours post-I/R in rats recovering for 2 days ($n=12$ for rats treated with HIFD with the renal vein occluded versus $n=11$ for rats given saline via the vena cava; * P value=0.001). Kidneys from rats after sham surgery, I/R + vena cava, or I/R + HIFD_{RV} 2 days after surgery were used for isolation of monocytes and FACS for the following populations: (B) total number CD4⁺ cells, (C) CD8⁺ cells, (D) total number of IL17⁺ cells, (E) CD4+IL17⁺ cells, and (F) CD8+IL17⁺ cells. (G) A line scan captures average RBC velocity in the capillary space comparing pre- and post-HIFD injection versus pre- and post-HIFD_{RV}. For FACS analysis, data are expressed as mean \pm SEM number of cells per gram kidney weight; *,\$ P <0.05 for sham versus *I/R + vena cava or \$I/R + HIFD_{RV}; # P <0.05 for I/R + vena cava versus I/R + HIFD_{RV} by paired t test.

Improvement of renal vascular perfusion in the setting of AKI is a potential therapy in the treatment of AKI. However, although vasodilator therapies have shown promise in preventing renal injury before ischemia, their ability to improve renal function after established AKI has been limited.^{39,40} Clinically, renal-dose dopamine has not translated to improvement in patients with AKI.^{6,41–46} However, as peritubular capillaries are among the first structures affected during an ischemic insult, it is likely that their impaired blood flow rates and lower hydrostatic pressure combine to promote leukocyte adherence and congestion.²⁰ Because vascular congestion occurs distal to the efferent arteriole and is a significant factor in reducing perfusion and driving the extension phase, it is reasonable that timely vascular therapies influencing preglomerular

vascular tone lack efficacy in treating established AKI. We hypothesized that an increase in hydrostatic pressure may disrupt vascular congestion, leading to the resolution of established AKI. High-pressure (66 \pm 5.74 mmHg) HIFD into the renal vein resulted in a near immediate reduction in serum creatinine (Figures 2A and 5A), an alleviation of microvascular rouleaux (Figures 2F and 3, B and C), and an improvement of RBC velocity (Figures 3D and 5G). HIFD therapy also improved tissue injury scores 4 days post-I/R (Figure 2, F–H). A striking result of our experiments is that a single intervention performed 24 hours after injury is capable of leading to sustained improvement in renal function and tissue morphology. This strongly underscores the benefit of resolving microvascular congestion post-AKI.

Whether HIFD is translatable to the clinical setting is unclear. This study used an invasive approach where isotonic saline injected retrograde into the renal vein improves renal function after I/R injury. Although this open, invasive procedure is not practicable to treat established human AKI, other intravascular approaches using endovascular catheters can effectively deliver solutions *via* retrograde delivery in large animal models and humans.^{47–52}

The proposed lack of no-reflow in large animal models as well as humans is often a point of contention with the use of various animal models in experimental AKI.^{53–57} However, several of these studies described a lack of the no-reflow phenomenon where renal blood flow returned to baseline levels very early (*e.g.*, 2 minutes) after reperfusion.^{55,56} This is consistent with rodent data, where blood flow returns to baseline levels early after reperfusion, but declines over time.^{1,58} Vascular congestion and peritubular capillary derangement manifesting hours and days after reperfusion are demonstrably important in the pathogenesis of AKI in large animal models and humans.^{26,52,57,59–63} For example, Mandal *et al.* demonstrated that I/R caused significant rouleaux formation in dogs, which was alleviated by splenectomy.⁶² Further, Solez *et al.* demonstrated that 63 of 66 cadaver kidneys from patients with AKI for >24 hours' duration had significant intravascular leukocyte accumulation.⁶³ Alleviation of vascular congestion and improvement of renal microvascular blood flow by HIFD demonstrates a potential mechanism that supports the concept of establishing full tissue level perfusion in patients with established AKI.

To determine if HIFD influenced leukocyte infiltration, we evaluated immune cell populations after surgery. In addition to improved perfusion, we hypothesized that the HIFD procedure reduces the inflammatory state post-I/R injury. That both innate and adaptive immune systems play a role in I/R injury is well established.⁶⁴ After I/R, the injured renal parenchymal cells facilitate the trafficking of, for instance, innate lymphoid cells like leukocytes, B cells, dendritic cells, and macrophages into the kidney.^{20,64–67} The balance between pro- and anti-inflammatory mediators significantly affects the extent of injury and reparative mechanisms.⁶⁴ Inflammation also causes anticoagulant production to be significantly decreased after ischemic AKI.⁶⁸ Several reports have indicated that T cells contribute to renal injury after I/R.^{28,66,69,70} Recently, Chan *et al.* and our group suggested that IL-17 cytokine plays an important role in AKI.^{28,71} Here we show that at 24 hours post-AKI, renal vein HIFD significantly decreases the number of infiltrating T cells (CD4+, CD8+), IL-17 cells (Figures 4 and 5), B cells (Table 1), and DC/Macs (Table 1), indicating that retrograde HIFD is a novel and effective treatment to reduce inflammation after injury. It is likely that these inflammatory cells or proinflammatory cytokines exit from kidney parenchyma leading to decreased cell infiltration. Additionally, HIFD increased the percentage of T regulatory cells, suggesting a shift from pro- to anti-inflammatory phenotype. Taken together, these data suggest that HIFD may improve renal function by improving vascular perfusion as well as decreasing the injurious effects of infiltrating leukocytes after injury is established.

In summary, data presented here demonstrate for the first time a novel approach to treating established AKI. In addition to treating established AKI, HIFD may have other additional advantages. Several pharmacologic agents that have been shown to prevent AKI have been employed or are in the pipeline for the treatment of established AKI, such as antiapoptosis/necrosis agents,^{72–75} free radical scavengers,^{76,77} antisepsis agents,^{78–81} anti-inflammatory drugs,^{82,83} loop diuretics,^{84,85} and vasodilators.^{6,14} In a recent review, Okusa has summarized the numerous clinical trial failures, where pharmacologic interventions are attempted after AKI is established.⁷ Our data suggest that a common cause of failure is a defect in target cell delivery of pharmacologic agents. The HIFD approach may prove effective where other attempts have failed in AKI therapy and prevention of CKD. Beyond isotonic saline, pharmacologic agents or small molecules (Figure 3C) that fail to reach kidneys effectively when given systemically may better treat AKI *via* HIFD.

CONCISE METHODS

Animal Care and Use

Male Sprague Dawley rats (Harlan Laboratories, Indianapolis, IN), with weights ranging from 225 to 300 g, were used for these studies. Rats had free access to standard rat chow and water throughout our studies. Experiments were conducted in accordance with the National Institutes of Health (NIH) Guidelines and were approved by the Indiana University School of Medicine Institutional Animal Care and Use Committee.

Rat Kidney I/R Injury Model

AKI was induced by procedures similar to those described previously⁸⁶ with modifications described subsequently. Rats were anesthetized with intraperitoneal injections of ketamine (100 mg/kg) with xylazine (5 mg/kg) and then placed on a heating pad to maintain physiologic temperature. For studies in which confocal images were conducted, acepromazine (1 mg/kg) was also included in the anesthesia. An abdominal midline incision was made and the right renal artery, vein, and ureter were ligated using 4–0 silk. The right kidney was bluntly dissected free and removed. Unilateral I/R was induced by occluding the left renal pedicle with microaneurism clamps (Fine Science Tools, Foster City, CA) for 40 minutes. At the end of the ischemic period, the clamp was removed to reinitiate renal blood flow. Upon visual confirmation of renal reperfusion, animals were allowed to fully recover from anesthesia.

HIFD

HIFD was conducted similarly to the method which facilitates plasmid delivery to rat kidneys¹² with modifications described subsequently. Twenty-four hours after I/R injury, rats were anesthetized under isoflurane and the left renal pedicle was exposed. The renal vein was bluntly dissected and then elevated with either 3–0 or 4–0 silk suture thread. The renal pedicle was occluded with a micro serraflaine clamp and 0.5 ml of saline was immediately injected retrograde into the vein (*i.e.*, toward the kidney) over a period of approximately 4 seconds, using a 30 gauge stainless steel needle attached to a 1 ml syringe, at the site between the suture and the kidney. Under these conditions, the kidney

transiently swells due to fluid injection. The needle was removed, and pressure was applied to the injection site using a cotton swab to induce hemostasis. The vascular clamp was removed to restore renal blood flow, and the total occlusion period was predetermined to equal 3 minutes. After this, the midline incision was closed and the animal was allowed to fully recover. In additional studies performed to examine the effect of renal vein occlusion during HIFD procedures, only the renal vein was occluded without clamping the renal artery (HIFDrv). Otherwise, HIFD was performed as described above.

In some experiments, renal venous pressure was measured simultaneous to HIFD. In these studies, a second 30 g needle shaft was removed from its hub and attached in parallel with the needle used for delivery of saline using Vetbond (3M), such that the tips of both needle shafts were closely opposed to each other, and both tips could be introduced and removed from the renal vein with minimal damage. The distal end of the needle was attached to a PE-10 polyethylene catheter tube, which was filled with heparinized saline, and connected to a fluid pressure transducer (World Precision Instruments, Sarasota, FL). Signals from the transducer were amplified with a Transbridge amplifier (World Precision Instruments) and acquired in real-time using data-acquisition software (Biopac Systems, Goleta, CA).

Materials

All fluorescent-tagged chemicals, with the exception of fluorescent-tagged dextran, were purchased from Molecular Probes–Thermo Scientific (Waltham, MA). Fluorescence-conjugated 150 kD dextran was purchased from TdB Consultancy (Upsalla, SW). Sterile saline was purchased from Baxter–Travenol (Deerfield, IL). Diaminobenzidine and lead acetate were purchased from Electron Microscopy Sciences (Hatfield, PA).

Serum Creatinine Measurements

At the indicated times, blood was obtained from rats under light isoflurane anesthesia *via* tail vein incisions. Blood was collected in 1 ml Eppendorf, heparin-treated tubes, centrifuged at 3000 g for 10 minutes, and the plasma stored at 4°C. Serum creatinine was measured using a Point Scientific QT 180 Analyzer and creatinine reagent kit (Point Scientific, Inc., Canton, MI) according to the manufacturer's specifications.

Fluorescence Cell and Tissue Markers

The following fluorescent probes were used in our intravital two-photon fluorescent imaging studies: 150 kD TRITC dextran (TdB Consultancy) and Hoechst 33342 (ThermoFisher Scientific, Waltham, MA). Each dextran solution was prepared by diluting 500 µl of a 20 mg/ml stock solution in 1 ml of saline. We also used 30–50 µl of Hoechst 33342 (Invitrogen, Carlsbad, CA) that was diluted in 0.5 ml saline.

Correlative Light and Electron Microscopy

Twenty-four hours after I/R injury, the animals were anesthetized with isoflurane, infusion catheters were placed in the carotid artery, and the rats were injected with Hoechst 33342 and 150 kD fluorescein-conjugated dextran (TdB Consultancy), as previously described.¹² Imaging was performed with a BioRad MRC 1024 two-photon confocal microscope attached to an inverted Nikon microscope.¹² When

an ROI was identified, a biopsy sample was taken using the micro-biopsy system (Leica Microsystems, Vienna, Austria). For these specimens, the sample holder was not dipped in hexadecane. The samples were quickly loaded into a slotted specimen holder using the transfer station. Any space left in the specimen holder was filled with hexadecane and frozen.

Biopsy samples of kidney were prepared for electron microscopy by freeze substitution and low-temperature embedding using a Leica EMPACT (Leica Microsystems, Vienna, Austria) High Pressure Freezer. Samples were frozen at 2100 bar with an average cooling rate of $-13,000^{\circ}\text{K s}^{-1}$. Once the samples were frozen they were stored in liquid nitrogen until they were ready for freeze substitution.

Freeze Substitution and Embedding

All samples were freeze-substituted using a Leica Automatic Freeze Substitution Unit (Leica Microsystems, Vienna, Austria). Samples were freeze-substituted in 0.01% osmium tetroxide, 0.1% gallium arsenide, 0.25% uranyl acetate in acetone, and embedded in LR Gold (Electron Microscopy Services, Hatfield, PA). The freeze substitution schedule was as follows; -90°C for 3 days, warmed to -25°C at 5°C/h , then at -25°C for 6 hours. Some of the samples were warmed to 0°C over a 2.5-hour period, rinsed with 100% acetone, warmed to room temperature, and infiltrated in 1:2 resin/acetone for 2 hours followed by 2:1 resin/acetone overnight. Samples were embedded and then polymerized at -20°C . Sections were cut with a Leica Ultracut UCT Ultramicrotome (Leica Microsystems, Vienna, Austria). Sections were imaged with an FEI electron microscope equipped with an AMT charged-coupled device camera.

Intravital Light Microscopy Assessment of Capillary Blood Flow, Vascular Permeability, and Hoechst 33342 Labeling

Twenty-four hours after renal I/R injury, isoflurane-anesthetized rats were prepared for intravital light microscopy as described above. A line scan was generated from the center of the vessel of interest continuously at a rate of 2 milliseconds per line for 1 second (1000 total lines). The scan measures flowing red blood cells, which do not take up dye and are therefore black. To analyze the scan, all channels of the line scan are merged into a single channel. This results in a vertical axis denoting time and a horizontal axis denoting the length of the scan, or distance. The velocity of the blood cells was determined using the dark lines which depict the movement of the blood cell along the scan over time. The flow velocity was determined by measuring the slope as described by Dunn *et al.*⁸⁸ and Lin *et al.*⁸⁹

A complementary approach was taken to measure vascular permeability after HIFD. Twenty-four hours after performing postnephrectomy, contralateral I/R injury, HIFD was performed on the remnant kidney. Twenty minutes after HIFD, 150 kD TRITC-conjugated dextran and Hoechst 33342 were injected *via* the tail vein. Intravital imaging was performed on the kidney at a rate of 2 milliseconds per line for a total of 5 minutes. Vascular permeability was determined by measuring the change in red channel fluorescence along a line perpendicular to a capillary wall. Sequential changes in fluorescent intensity over time were used to determine the rate of high-mol wt dextran entry into the interstitial compartment. Ten fields were studied for each animal and

statistical significance was determined at a *P* value <0.05 using paired *t* test.

To evaluate changes in Hoechst 33342 signal, 512 × 512 image scans were collected with simultaneous acquisition of 420 and 514 nm wavelengths at 1 scan/s using 800 nm excitation light in two-photon mode. Thirty scans were acquired from each animal with random field selection. Images were acquired 24 hours post-I/R injury and 20 minutes after HIFD in post-I/R injury rats. Images were collected from sham-operated rats. Image intensity values were obtained by defining a circular ROI. Average intensity values were obtained by placing the ROI over nuclei in all cells in a field using ImageJ (NIH).^{90,91} Statistical significance was determined using paired *t* test.

Evaluation of Renal Tubular Damage and RBC Congestion

Renal tubular damage was evaluated from formalin-fixed paraffin-embedded samples stained using hematoxylin and eosin. Six random images (three cortex, three outer medulla) were obtained using a Leica DMLB microscope (Scientific Instruments, Columbus, OH) using a 20× objective. For each kidney, an average of 60 tubules were scored from images by an observer who was blinded to the treatments using a modified one to four scoring system described previously.⁹² Data presented are on the basis of the average score per tubule corresponding to each animal.

RBC congestion was analyzed using ImageJ software, whereby regions of interest were identified visually and used to calculate percentage surface area.

Assessment of Renal Infiltrating Cells

Harvested kidneys were minced and digested with liberase (2 µg/ml; Roche, Basel, Switzerland) for 15 minutes at 37°C using Gentle MACs (Miltenyi, San Diego, CA). Digested tissue was filtered through a 100 µm filter mesh and washed with medium. Mononuclear cells were separated by Percoll (Sigma-Aldrich, St. Louis, MO) and counted by hemocytometer. To evaluate T lymphocytes, the cells were stained with antibodies against rat CD4 (PE-Cy7), CD8a (Alexa 647), and CD161 (PE-Cy7). To evaluate the T helper subtype, the cells were permeabilized and stained with antibodies against cytokines such as IFN-γ (FITC; Th1), IL-4 (PE; Th2), and IL-17 (FITC; Th17). To evaluate regulatory T cells, mononuclear cells were stained with either CD4 or CD4 along with Foxp3 (PE). To evaluate B cells and DC/Mac mononuclear cells were labeled with antibodies against RTIB (FITC) and Cd11b/c (PE), respectively. Fluorescence was measured using flow cytometry (FACSCalibur; BD Biosciences, San Jose, CA) and dot plots were analyzed using Flowjo software (Tree Star, Ashland, OR). Lymphocyte gating strategy was identical to that shown previously.²⁸ The data are expressed as a total number of the specific cell population per gram of kidney.

Statistical Analyses

Statistical analysis of changes in serum creatinine was performed by paired *t* test with significance determined at a *P* value <0.05. Statistical analysis for RBC flow velocity and Hoechst intensity before and after HIFD was performed by paired *t* test with significance determined at a *P* value <0.05.

ACKNOWLEDGMENTS

The authors thank the staff of the Indiana Center for Biological Microscopy for their expert advice and support.

R.L.B. is supported by Veteran's Administration Merit Award BX001736. D.P.B. is supported by National Institutes of Health DK063114. J.A.C. is supported by the National Institutes of Health T32 HL07995. B.A.M. is supported by the O'Brien Center for Advanced Renal Microscopic Analysis at the Indiana Center for Biological Microscopy. B.A.M.'s grant support is from the National Institutes of Health (DK091623 and DK079312) and support from the Veterans Administration is through a Merit Review award.

DISCLOSURES

R.L.B. is a scientific officer for Rene Medical and is a paid consultant to Mitobridge.

REFERENCES

- Basile DP, Anderson MD, Sutton TA: Pathophysiology of acute kidney injury. *Compr Physiol* 2: 1303–1353, 2012
- Sutton TA, Fisher CJ, Molitoris BA: Microvascular endothelial injury and dysfunction during ischemic acute renal failure. *Kidney Int* 62: 1539–1549, 2002
- Molitoris BA, Sutton TA: Endothelial injury and dysfunction: Role in the extension phase of acute renal failure. *Kidney Int* 66: 496–499, 2004
- Brodsky SV, Yamamoto T, Tada T, Kim B, Chen J, Kajiyama F, Goligorsky MS: Endothelial dysfunction in ischemic acute renal failure: Rescue by transplanted endothelial cells. *Am J Physiol Renal Physiol* 282: F1140–F1149, 2002
- Fry AC, Farrington K: Management of acute renal failure. *Postgrad Med J* 82: 106–116, 2006
- Denton MD, Chertow GM, Brady HR: "Renal-dose" dopamine for the treatment of acute renal failure: Scientific rationale, experimental studies and clinical trials. *Kidney Int* 50: 4–14, 1996
- Chopra TA, Brooks CH, Okusa MD: Acute kidney injury prevention. *Contrib Nephrol* 187: 9–23, 2016
- Yamamoto T, Tada T, Brodsky SV, Tanaka H, Noiri E, Kajiyama F, Goligorsky MS: Intravital videomicroscopy of peritubular capillaries in renal ischemia. *Am J Physiol Renal Physiol* 282: F1150–F1155, 2002
- Summers WK, Jamison RL: The no reflow phenomenon in renal ischemia. *Lab Invest* 25: 635–643, 1971
- Nakano D, Doi K, Kitamura H, Kuwabara T, Mori K, Mukoyama M, Nishiyama A: Reduction of tubular flow rate as a mechanism of oliguria in the early phase of endotoxemia revealed by intravital imaging. *J Am Soc Nephrol* 26: 3035–3044, 2015
- Wu L, Tiwari MM, Messer KJ, Holthoff JH, Gokden N, Brock RW, Mayeux PR: Peritubular capillary dysfunction and renal tubular epithelial cell stress following lipopolysaccharide administration in mice. *Am J Physiol Renal Physiol* 292: F261–F268, 2007
- Corrion PR, Rhodes GJ, Leonard EC, Basile DP, Gattone VH 2nd, Bacallao RL, Atkinson SJ: A method to facilitate and monitor expression of exogenous genes in the rat kidney using plasmid and viral vectors. *Am J Physiol Renal Physiol* 304: F1217–F1229, 2013
- Sutton TA, Mang HE, Campos SB, Sandoval RM, Yoder MC, Molitoris BA: Injury of the renal microvascular endothelium alters barrier function after ischemia. *Am J Physiol Renal Physiol* 285: F191–F198, 2003
- Conger JD, Robinette JB, Schrier RW: Smooth muscle calcium and endothelium-derived relaxing factor in the abnormal vascular responses of acute renal failure. *J Clin Invest* 82: 532–537, 1988

15. Mason J, Torhorst J, Welsch J: Role of the medullary perfusion defect in the pathogenesis of ischemic renal failure. *Kidney Int* 26: 283–293, 1984
16. Luke DR, Berens KL, Verani RR: Role of vascular decongestion in ischemic acute renal failure defined by postinsult administration of pentoxifylline. *Ren Fail* 11: 187–194, 1989–1990
17. Richards WL, Song MK, Krutzsch H, Evarts RP, Marsden E, Thorgeirsson SS: Measurement of cell proliferation in microculture using Hoechst 33342 for the rapid semiautomated microfluorimetric determination of chromatin DNA. *Exp Cell Res* 159: 235–246, 1985
18. Kinsey GR, Okusa MD: Expanding role of T cells in acute kidney injury. *Curr Opin Nephrol Hypertens* 23: 9–16, 2014
19. Sharfuddin AA, Molitoris BA: Pathophysiology of ischemic acute kidney injury. *Nat Rev Nephrol* 7: 189–200, 2011
20. Rabb H, O'Meara YM, Maderna P, Coleman P, Brady HR: Leukocytes, cell adhesion molecules and ischemic acute renal failure. *Kidney Int* 51: 1463–1468, 1997
21. Lee S, Huen S, Nishio H, Nishio S, Lee HK, Choi B-S, Ruhrberg C, Cantley LG: Distinct macrophage phenotypes contribute to kidney injury and repair. *J Am Soc Nephrol* 22: 317–326, 2011
22. Akcay A, Nguyen Q, Edelstein CL: Mediators of inflammation in acute kidney injury. *Mediators Inflamm* 2009: 137072, 2009
23. Ysebaert DK, De Greef KE, De Beuf A, Van Rompay AR, Vercauteren S, Persy VP, De Broe ME: T cells as mediators in renal ischemia/reperfusion injury. *Kidney Int* 66: 491–496, 2004
24. Yokota N, Daniels F, Crosson J, Rabb H: Protective effect of T cell depletion in murine renal ischemia-reperfusion injury. *Transplantation* 74: 759–763, 2002
25. Day YJ, Huang L, Ye H, Li L, Linden J, Okusa MD: Renal ischemia-reperfusion injury and adenosine 2A receptor-mediated tissue protection: The role of CD4+ T cells and IFN-gamma. *J Immunol* 176: 3108–3114, 2006
26. Friedewald JJ, Rabb H: Inflammatory cells in ischemic acute renal failure. *Kidney Int* 66: 486–491, 2004
27. Ysebaert DK, De Greef KE, Vercauteren SR, Ghielli M, Verpooten GA, Eyskens EJ, De Broe ME: Identification and kinetics of leukocytes after severe ischaemia/reperfusion renal injury. *Nephrol Dial Transplant* 15: 1562–1574, 2000
28. Mehrotra P, Patel JB, Ivancic CM, Collett JA, Basile DP: Th-17 cell activation in response to high salt following acute kidney injury is associated with progressive fibrosis and attenuated by AT-1R antagonism. *Kidney Int* 88: 776–784, 2015
29. Molitoris BA, Sandoval R, Sutton TA: Endothelial injury and dysfunction in ischemic acute renal failure. *Crit Care Med* 30[Suppl]: S235–S240, 2002
30. Fuller TF, Sattler B, Binder L, Vetterlein F, Ringe B, Lorf T: Reduction of severe ischemia/reperfusion injury in rat kidney grafts by a soluble P-selectin glycoprotein ligand. *Transplantation* 72: 216–222, 2001
31. Kelly KJ, Williams WW Jr., Colvin RB, Bonventre JV: Antibody to intercellular adhesion molecule 1 protects the kidney against ischemic injury. *Proc Natl Acad Sci USA* 91: 812–816, 1994
32. Haug CE, Colvin RB, Delmonico FL, Auchincloss Jr. H, Tolkkoff-Rubin N, Preffer FI, Rothlein R, Norris S, Scharschmidt L, Cosimi AB: A phase I trial of immunosuppression with anti-ICAM-1 (CD54) mAb in renal allograft recipients. *Transplantation* 55: 766–772; discussion 772–763, 1993
33. Ghielli M, Verstrepen WA, De Greef KE, Helbert MH, Ysebaert DK, Nouwen EJ, De Broe ME: Antibodies to both ICAM-1 and LFA-1 do not protect the kidney against toxic (HgCl₂) injury. *Kidney Int* 58: 1121–1134, 2000
34. Basile DP: Rarefaction of peritubular capillaries following ischemic acute renal failure: A potential factor predisposing to progressive nephropathy. *Curr Opin Nephrol Hypertens* 13: 1–7, 2004
35. Olof P, Hellberg A, Källskog O, Wolgast M: Red cell trapping and postischemic renal blood flow. Differences between the cortex, outer and inner medulla. *Kidney Int* 40: 625–631, 1991
36. Sharfuddin AA, Sandoval RM, Berg DT, McDougal GE, Campos SB, Phillips CL, Jones BE, Gupta A, Grinnell BW, Molitoris BA: Soluble thrombomodulin protects ischemic kidneys. *J Am Soc Nephrol* 20: 524–534, 2009
37. Solez K, Kramer EC, Fox JA, Heptinstall RH: Medullary plasma flow and intravascular leukocyte accumulation in acute renal failure. *Kidney Int* 6: 24–37, 1974
38. Hellberg PO, Källskog O, Wolgast M: Nephron function in the early phase of ischemic renal failure. Significance of erythrocyte trapping. *Kidney Int* 38: 432–439, 1990
39. Basile DP, Yoder MC: Renal endothelial dysfunction in acute kidney ischemia reperfusion injury. *Cardiovasc Hematol Disord Drug Targets* 14: 3–14, 2014
40. Urbschat A, Rupprecht K, Zacharowski K, Obermüller N, Scheller B, Holfeld J, Tepeköylü C, Hofmann R, Paulus P: Combined peri-ischemic administration of B₂B15-42 in treating ischemia reperfusion injury of the mouse kidney. *Microvasc Res* 101: 48–54, 2015
41. Power DA, Duggan J, Brady HR: Renal-dose (low-dose) dopamine for the treatment of sepsis-related and other forms of acute renal failure: Ineffective and probably dangerous. *Clin Exp Pharmacol Physiol Suppl* 26: S23–S28, 1999
42. Lameire N, van Biesen W, Hoste E, Vanholder R: The prevention of acute kidney injury an in-depth narrative review: Part 2: Drugs in the prevention of acute kidney injury. *NDT Plus* 2: 1–10, 2009
43. Bellomo R, Chapman M, Finfer S, Hickling K, Myburgh J; Australian and New Zealand Intensive Care Society (ANZICS) Clinical Trials Group: Low-dose dopamine in patients with early renal dysfunction: A placebo-controlled randomised trial. *Lancet* 356: 2139–2143, 2000
44. Burton CJ, Tomson CRV: Can the use of low-dose dopamine for treatment of acute renal failure be justified? *Postgrad Med J* 75: 269–274, 1999
45. Friedrich JO, Adhikari N, Herridge MS, Beyene J: Meta-analysis: Low-dose dopamine increases urine output but does not prevent renal dysfunction or death. *Ann Intern Med* 142: 510–524, 2005
46. Kellum JA, M Decker J: Use of dopamine in acute renal failure: A meta-analysis. *Crit Care Med* 29: 1526–1531, 2001
47. Bothe W: Retrograde administration. *Multimedia Manual of Cardio-Thoracic Surgery* 2005. Available at <http://mmcts.oxfordjournals.org/content/2005/0809/mmcts.2004.000711.full>. Accessed January 1, 2005
48. Giordano FJ: Retrograde coronary perfusion: A superior route to deliver therapeutics to the heart?*. *J Am Coll Cardiol* 42: 1129–1131, 2003
49. Hong SJ, Hou D, Brinton TJ, Johnstone B, Feng D, Rogers P, Fearon WF, Yock P, March KL: Intracoronary and retrograde coronary venous myocardial delivery of adipose-derived stem cells in swine infarction lead to transient myocardial trapping with predominant pulmonary redistribution. *Catheter Cardiovasc Interv* 83: E17–E25, 2014
50. Youssef EA-S, Zhang P, Rogers P, Tremble P, Rokovich J, Johnstone B, March KL, Hou D: 934. Comparing two modalities of myocardial gene delivery: Percutaneous retrograde coronary venous delivery and intramyocardial injection. *Mol Ther* 9: S357–S358, 2004
51. Paniagua D, Condado JA, Besso J, Vélez M, Burger B, Bibbo S, Cedeno D, Acquatella H, Mejia C, Induni E, Fish RD: First human case of retrograde transcatheter implantation of an aortic valve prosthesis. *Tex Heart Inst J* 32: 393–398, 2005
52. Bragadottir G, Redfors B, Ricksten S-E: Mannitol increases renal blood flow and maintains filtration fraction and oxygenation in postoperative acute kidney injury: A prospective interventional study. *Crit Care* 16: R159, 2012
53. Okusa MD, Rosner MH, Kellum JA, Ronco C; Acute Dialysis Quality Initiative XIII Workgroup: Therapeutic targets of human AKI: Harmonizing human and animal AKI. *J Am Soc Nephrol* 27: 44–48, 2016
54. Lieberthal W, Nigam SK: Acute renal failure. II. Experimental models of acute renal failure: Imperfect but indispensable. *Am J Physiol Renal Physiol* 278: F1–F12, 2000
55. Riley AL, Alexander EA, Migdal S, Levinsky NG: The effect of ischemia on renal blood flow in the dog. *Kidney Int* 7: 27–34, 1975
56. Parekh DJ, Weinberg JM, Ercole B, Torkko KC, Hilton W, Bennett M, Devarajan P, Venkatachalam MA: Tolerance of the human kidney to isolated controlled ischemia. *J Am Soc Nephrol* 24: 506–517, 2013

57. Bálint P, Szöcs E: Intrarenal hemodynamics following temporary occlusion of the renal artery in the dog. *Kidney Int Suppl* 6: S128–S136, 1976
58. Karlberg L, Källskog O, Norlén BJ, Wolgast M: Postischemic renal failure. Intrarenal blood flow and functional characteristics in the recovery phase. *Acta Physiol Scand* 115: 1–10, 1982
59. Vats A, Mauer M, Burke BA, Weiss RA, Chavers BM: Delayed acute renal failure in post-transplant period in young children from unexplained etiology. *Pediatr Nephrol* 11: 531–536, 1997
60. Lerolle N, Nochy D, Guérot E, Bruneval P, Fagon JY, Diehl JL, Hill G: Histopathology of septic shock induced acute kidney injury: Apoptosis and leukocytic infiltration. *Intensive Care Med* 36: 471–478, 2010
61. Heyman SN, Rosenberger C, Rosen S: Experimental ischemia-reperfusion: Biases and myths—the proximal vs. distal hypoxic tubular injury debate revisited. *Kidney Int* 77: 9–16, 2010
62. Mandal AK, Taylor CA, Bell RD, Hillman NM, Jarnot MD, Cunningham JD, Phillips LG: Erythrocyte deformation in ischemic acute tubular necrosis and amelioration by splenectomy in the dog. *Lab Invest* 65: 566–576, 1991
63. Solez K, Kramer E, Heptinstall RH: Pathology of acute renal-failure-leukocyte accumulation in vasa recta. *Am J Pathol* 74: 31a, 1974
64. Rabb H, Griffin MD, McKay DB, Swaminathan S, Pickkers P, Rosner MH, Kellum JA, Ronco C; Acute Dialysis Quality Initiative Consensus XIII Work Group: Inflammation in AKI: Current understanding, key questions, and knowledge gaps. *J Am Soc Nephrol* 27: 371–379, 2016
65. Kelley VR: Leukocyte-renal epithelial cell interactions regulate lupus nephritis. *Semin Nephrol* 27: 59–68, 2007
66. Rabb H, Daniels F, O'Donnell M, Haq M, Saba SR, Keane W, Tang WW: Pathophysiological role of T lymphocytes in renal ischemia-reperfusion injury in mice. *Am J Physiol Renal Physiol* 279: F525–F531, 2000
67. Jang HR, Rabb H: Immune cells in experimental acute kidney injury. *Nat Rev Nephrol* 11: 88–101, 2015
68. Brohi K, Cohen MJ, Ganter MT, Matthay MA, Mackersie RC, Pittet JF: Acute traumatic coagulopathy: Initiated by hypoperfusion? Modulated through the protein C pathway? *Ann Surg* 245: 812–818, 2007
69. De Greef KE, Ysebaert DK, Dauwe S, Persy V, Vercauteren SR, Mey D, De Broe ME: Anti-B7-1 blocks mononuclear cell adherence in vasa recta after ischemia. *Kidney Int* 60: 1415–1427, 2001
70. Burne MJ, Daniels F, El Ghadour A, Mauiyyedi S, Colvin RB, O'Donnell MP, Rabb H: Identification of the CD4(+) T cell as a major pathogenic factor in ischemic acute renal failure. *J Clin Invest* 108: 1283–1290, 2001
71. Chan AJ, Alikhan MA, Odobasic D, Gan PY, Khouri MB, Steinmetz OM, Mansell AS, Kitching AR, Holdsworth SR, Summers SA: Innate IL-17A-producing leukocytes promote acute kidney injury via inflammasome and Toll-like receptor activation. *Am J Pathol* 184: 1411–1418, 2014
72. Daemen MA, van 't Veer C, Denecker G, Heemskerk VH, Wolfs TG, Clauss M, Vandebaele P, Buurman WA: Inhibition of apoptosis induced by ischemia-reperfusion prevents inflammation. *J Clin Invest* 104: 541–549, 1999
73. Kelly KJ, Sutton TA, Weathered N, Ray N, Caldwell EJ, Plotkin Z, Dagher PC: Minocycline inhibits apoptosis and inflammation in a rat model of ischemic renal injury. *Am J Physiol Renal Physiol* 287: F760–F766, 2004
74. Kelly KJ, Plotkin Z, Vulgamott SL, Dagher PC: P53 mediates the apoptotic response to GTP depletion after renal ischemia-reperfusion: Protective role of a p53 inhibitor. *J Am Soc Nephrol* 14: 128–138, 2003
75. Chatterjee PK, Chatterjee BE, Pedersen H, Sivarajah A, McDonald MC, Mota-Filipe H, Brown PA, Stewart KN, Cuzzocrea S, Threadgill MD, Thiemermann C: 5-Aminoisoquinolinone reduces renal injury and dysfunction caused by experimental ischemia/reperfusion. *Kidney Int* 65: 499–509, 2004
76. Walker PD, Shah SV: Evidence suggesting a role for hydroxyl radical in gentamicin-induced acute renal failure in rats. *J Clin Invest* 81: 334–341, 1988
77. Baliga R, Ueda N, Walker PD, Shah SV: Oxidant mechanisms in toxic acute renal failure. *Drug Metab Rev* 31: 971–997, 1999
78. Ulloa L, Ochani M, Yang H, Tanovic M, Halperin D, Yang R, Czura CJ, Fink MP, Tracey KJ: Ethyl pyruvate prevents lethality in mice with established lethal sepsis and systemic inflammation. *Proc Natl Acad Sci USA* 99: 12351–12356, 2002
79. Miyaji T, Hu X, Yuen PS, Muramatsu Y, Iyer S, Hewitt SM, Star RA: Ethyl pyruvate decreases sepsis-induced acute renal failure and multiple organ damage in aged mice. *Kidney Int* 64: 1620–1631, 2003
80. Grey ST, Tsuchida A, Hau H, Orthner CL, Salem HH, Hancock WW: Selective inhibitory effects of the anticoagulant activated protein C on the responses of human mononuclear phagocytes to LPS, IFN-gamma, or phorbol ester. *J Immunol* 153: 3664–3672, 1994
81. van den Berghe G, Wouters P, Weekers F, Verwaest C, Bruyninx F, Schetz M, Vlasselaers D, Ferdinand P, Lauwers P, Bouillon R: Intensive insulin therapy in critically ill patients. *N Engl J Med* 345: 1359–1367, 2001
82. Linden J: Molecular approach to adenosine receptors: Receptor-mediated mechanisms of tissue protection. *Annu Rev Pharmacol Toxicol* 41: 775–787, 2001
83. Okusa MD, Linden J, Macdonald T, Huang L: Selective A2A adenosine receptor activation reduces ischemia-reperfusion injury in rat kidney. *Am J Physiol* 277: F404–F412, 1999
84. Ho KM, Power BM: Benefits and risks of furosemide in acute kidney injury. *Anesthesia* 65: 283–293, 2010
85. Karajala V, Mansour W, Kellum JA: Diuretics in acute kidney injury. *Minerva Anestesiol* 75: 251–257, 2009
86. Basile DP, Friedrich JL, Spahic J, Knipe N, Mang H, Leonard EC, Changizi-Ashtiyani S, Bacallao RL, Molitoris BA, Sutton TA: Impaired endothelial proliferation and mesenchymal transition contribute to vascular rarefaction following acute kidney injury. *Am J Physiol Renal Physiol* 300: F721–F733, 2011
87. Vella F: *Textbook of Clinical Chemistry*, edited by Tietz NW, Philadelphia, WB Saunders, 1986, pp 1919
88. Dunn AK, Bolay H, Moskowitz MA, Boas DA: Dynamic imaging of cerebral blood flow using laser speckle. *J Cereb Blood Flow Metab* 21: 195–201, 2001
89. Lin W-C, Wu C-C, Huang T-C, Lin W-C, Chiu BY-C, Liu R-S, Lin K-P: Red blood cell velocity measurement in rodent tumor model: An in vivo microscopic study. *J Med Biol Eng* 32: 97–102, 2011
90. Schneider CA, Rasband WS, Eliceiri KW: NIH Image to ImageJ: 25 years of image analysis. *Nat Methods* 9: 671–675, 2012
91. Abràmoff MD, Magalhães PJ, Ram SJ: Image processing with ImageJ. *Biophoton Int* 11: 36–42, 2004
92. Basile DP, Dwinell MR, Wang SJ, Shames BD, Donohoe DL, Chen S, Sreedharan R, Van Why SK: Chromosome substitution modulates resistance to ischemia reperfusion injury in Brown Norway rats. *Kidney Int* 83: 242–250, 2013

This article contains supplemental material online at <http://jasn.asnjournals.org/lookup/suppl/doi:10.1681/ASN.2016040404/-DCSupplemental>.